

Solution-processed bulk heterojunction photovoltaic devices based on poly(2-methoxy,5-octoxy)-1,4-phenylenevinylene-multiwalled carbon nanotubes/PbSe quantum dots bilayer

Yiyu Feng, Daqin Yun, Xuequan Zhang, and Wei Feng

Citation: *Appl. Phys. Lett.* **96**, 093301 (2010); doi: 10.1063/1.3337100

View online: <http://dx.doi.org/10.1063/1.3337100>

View Table of Contents: <http://apl.aip.org/resource/1/APPLAB/v96/i9>

Published by the [American Institute of Physics](http://www.aip.org).

Additional information on *Appl. Phys. Lett.*

Journal Homepage: <http://apl.aip.org/>

Journal Information: http://apl.aip.org/about/about_the_journal

Top downloads: http://apl.aip.org/features/most_downloaded

Information for Authors: <http://apl.aip.org/authors>

ADVERTISEMENT



Goodfellow
metals • ceramics • polymers • composites
70,000 products
450 different materials
small quantities fast

www.goodfellowusa.com

Solution-processed bulk heterojunction photovoltaic devices based on poly(2-methoxy,5-octoxy)-1,4-phenylenevinylene-multiwalled carbon nanotubes/PbSe quantum dots bilayer

Yiyu Feng,¹ Daqin Yun,² Xuequan Zhang,¹ and Wei Feng^{1,a)}

¹School of Materials Science and Engineering, Tianjin Key Laboratory of Composite and Functional Materials, Tianjin University, Tianjin 300072, People's Republic of China

²School of Electrical and Information Engineering, Xi'an Jiaotong University, Xi'an 710049, People's Republic of China

(Received 16 October 2009; accepted 4 February 2010; published online 1 March 2010)

A solution-processed bulk heterojunction photovoltaic cell was fabricated based on poly[(2-methoxy,5-octoxy)-1,4-phenylenevinylene](MOPPV)-multiwalled carbon nanotubes (MWNT)/spherical PbSe quantum dots bilayer. Surface morphology shows the interpenetrating network of well-dispersed MWNT in MOPPV matrix. Blueshifted band in absorption and photoluminescence spectra indicate the strong electron interaction between MWNT and MOPPV. A marked twofold increase in short-circuit current (1.71 mA/cm²) and power-conversion efficiency (0.40%) of ITO/MOPPV-MWNT:phenyl-C61-butyric acid methyl ester (PCBM)/PbSe/Al devices was achieved compared with that without MWNT. Results indicate that the enhanced performance was contributed by high photocurrent due to efficient exciton dissociation, charge transfer, and mobility in MWNT pathway. © 2010 American Institute of Physics. [doi:10.1063/1.3337100]

Solution-processed organic polymeric photovoltaics (OPV) were distinguished as an attractive flexible alternative to rigid silicon devices due to low-cost, easy-processing, and up-scale production.¹ However, the intrinsic low carrier transport of conjugated polymers and ineffective exciton dissociation was essentially responsible for the low photocurrent.² The development of photoinduced charge transfer provided a molecular approach to optimize the photoconversion process. A dramatic enhancement in photovoltaic performance was achieved by the integration of carbon nanotubes (CNT) into OPV due to the efficient charge transfer and transport. Kymakis and Amaratunga³ reported two orders of magnitude in photocurrent of the device based on single-walled carbon nanotubes (SWNT)/poly(3-octylthiophene) blend. This result was supported by Pradhan's study⁴ in which multiwalled carbon nanotubes (MWNT)/poly(3-hexylthiophene) (P3HT) network serving as a direct pathway for holes transport led to a marked increase in both open-circuit voltage (V_{oc}) and short-circuit current (J_{sc}). Recently, OPV based on solution processed quantum dots (QDs), polymers received the increasing attention due to the effective collection of photons at the infrared region and high intrinsic carrier mobility of QDs.⁵ Schaller *et al.*⁶ reported multiple exciton generation in PbSe QDs by absorbing a photon. Koleilat *et al.*⁷ found the diffusion of electron and holes hundreds of nanometers through PbSe QDs led to high external quantum efficiencies of the devices. The broad photon absorption, fast exciton dissociation at the polymer/QDs interface and enhanced electron transport promisingly resulted in the superior photovoltaic performance exceeding the Shockley/Queisser limit

Among several methods to prepare CNT/polymer hybrids, covalent bonding is effective to disperse nanotubes

uniformly at molecular level in polymer matrix.⁸ The continuous pathway for charge collection and transport reasonably results in high photovoltaic performance. Compared with P3HT, the low photocurrent of poly[(2-methoxy,5-octoxy)-1,4-phenylenevinylene] (MOPPV) OPV was attributed to low carrier mobility.⁹ In this paper, MWNT with high carrier mobility, which primarily acts as a metallic conductor, was utilized to functionalize MOPPV by covalent attachment. A solution-processed bulk heterojunction OPV based on MOPPV-MWNT/PbSe bilayer shows twofold increase in current (1.71 mA/cm²) and efficiency (0.40%) compared with the device without MWNT. High performance of MOPPV-MWNT OPV depends on the enhancement in photocurrent arising from efficient charge transfer and high carrier mobility.

Figure 1 shows the x-ray diffraction (XRD) pattern of PbSe film prepared by a colloidal chemical method.¹⁰ Results indicate that the crystal structure of PbSe QDs is the rock-salt phase. Uniform spherical PbSe nanocrystal with ~6 nm diameter [transmission electron microscopy (TEM) image, inset of Fig. 1] is stabilized by a capping layer of organic molecules coordinated to the Pb atoms. Individual

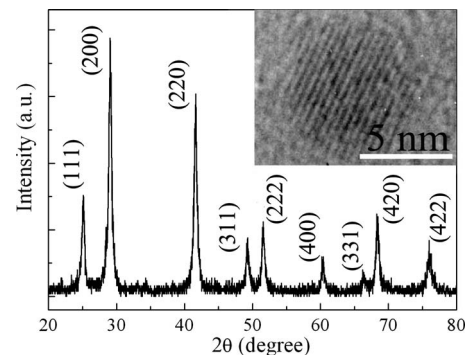


FIG. 1. XRD pattern of PbSe nanocrystals. Inset: TEM image of PbSe QDs.

^{a)}Author to whom correspondence should be addressed. Electronic mail: weifeng@tju.edu.cn.

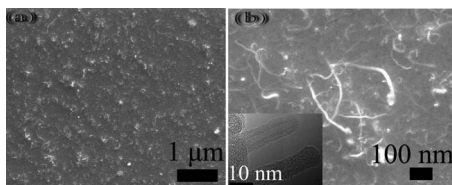


FIG. 2. (a) Low and (b) high-resolution SEM images of MOPPV-MWNT film. Inset: TEM image of individual MOPPV-MWNT.

MOPPV-MWNT synthesized by covalent attachment and *in situ* polymerization⁹ was observed by TEM. Inset of Fig. 2(b) shows an essentially molecular core-shell nanostructure with MWNT core in the center encapsulated in long polymers. The robust polymer layers on the sidewall debundled the nanotubes, facilitating exciton dissociation, and charge transfer.

The surface morphology of MOPPV-MWNT film was observed by scanning electron microscope (SEM). The uniform continuous film [Fig. 2(a)] indicates typical surface morphology of nanotubes wrapped in polymers matrix. High-resolution images [Fig. 2(b)] shows random and curled MWNT dispersed in MOPPV matrix constructs network structure of porous film. This structure enables the infiltration of PbSe into the vacancy of polymers network leading to the effective exciton dissociation at the interface between QDs and polymers.

Figure 3 shows the ultraviolet-visible-near infrared (UV-vis-NIR) absorption spectra of PbSe QDs (triangles), MOPPV (circles), and MOPPV-MWNT (squares), respectively. PbSe exhibit an exciton absorption band at 1686 nm (0.73 eV). This near-infrared peak indicates 6–7 nm PbSe QDs,¹¹ which is in consistency with XRD and TEM results. MOPPV-MWNT mostly absorbs UV and visible light with the maximum at 482 nm attributed to π - π^* electronic transition of MOPPV. This band is a 10 nm blueshift from that of MOPPV due to shorted MOPPV conjugation chain. The blueshifted band in the excited state was confirmed by photoluminescence (PL) spectra, in which the luminescent band of MOPPV-MWNT film blueshifted by 7 nm from that of MOPPV. A dramatic quenching luminescent band centered at 530 nm with the shoulder at 630 nm was clearly shown in PL spectra of MOPPV-MWNT (inset of Fig. 3). This quenching luminescence arose from exciton dissociation prior to the radiative recombination between MOPPV and MWNT.¹² Surface morphology observation and optical spectra demon-

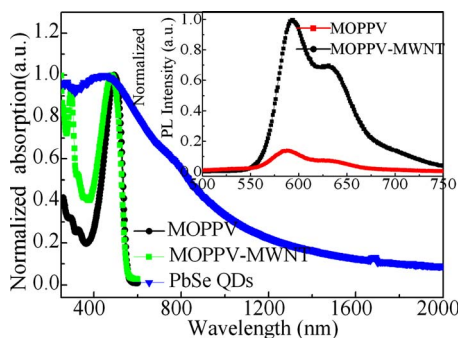


FIG. 3. (Color online) UV-vis-NIR absorption spectra of PbSe QDs (triangles), MOPPV (circles), and MOPPV-MWNT (squares) in chloroform. Inset: Normalized PL spectra of MOPPV (squares) and MOPPV-MWNT (circles) film excited at 350 nm.

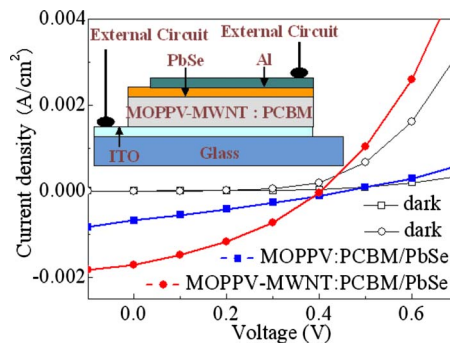


FIG. 4. (Color online) Current-voltage characteristics of OPV with active layer of MOPPV-MWNT:PCBM/PbSe (circles) and MOPPV:PCBM/PbSe (squares) under dark (hollow) and white light illuminations (solid) of 60 mW/cm². Inset: Schematic structure of bulk-heterojunction OPV.

strate that well-dispersed MWNT form interpenetrating network in polymeric matrix.

Bulk-heterojunction OPV was fabricated and illustrated in the inset of Fig. 4. The indium tin oxide (ITO) ($\sim 20 \Omega \text{ sq}^{-1}$) layer was partially etched and cleaned in an ultrasonic bath with actone, isopropanol, and deionized water. The MOPPV-MWNT/PCBM thin film ($\sim 100 \text{ nm}$) was spin-coated on ITO using chloroform solution with a concentration of 10 mg/ml. The brief annealing of the film for 15 min at 100 °C removes the residual solvent. Subsequently, the PbSe QDs layer was spin-coated from a filtered pyridine solution to form the $\sim 100 \text{ nm}$ film on the MOPPV-MWNT/PCBM layer and annealing at 150 °C for 30 min. Finally, an aluminum top electrode was fabricated using thermal evaporation in a vacuum of 2×10^{-6} Torr through a shadow mask. The active area of the two devices is about 0.1 cm².

Figure 4 presents current-voltage (*I*-*V*) characteristics of OPV with the active layer of MOPPV-MWNT:PCBM/PbSe (circles) and MOPPV:PCBM/PbSe (squares) under dark (hollow) and white light illuminations (solid) measured with a Keithley 236 source-measure unit (AM 1.5). A marked twofold increase in J_{sc} of 1.71 mA/cm² and PCE (η) of 0.40% with V_{oc} of 0.406 V and fill factor (*FF*) of 35% is achieved by OPV with ITO/MOPPV-MWNT:PCBM/PbSe/Al compared with the device without MWNT which shows V_{oc} of 0.457 V, J_{sc} of 0.688 mA/cm² and fill factor (*FF*) of 27%, resulting in low η of 0.14%. Short-circuit current and PCE of OPV based on MOPPV-MWNT/PbSe bilayer are twice higher than those of PbSe/P3HT device.¹³

High photovoltaic performance is enhanced by inserting MWNT interpenetrating network in polymer matrix for efficient charge transfer. The essential limitation of conjugated polymers is low carrier mobility (typically 10^{-5} – $0.1 \text{ cm}^2/\text{V s}$) and small exciton diffusion length ($L_D \approx 5$ – 20 nm).² Unbalanced charge transport and holes accumulation results in the space-charge limited photocurrent and low efficiency.¹⁴ Electrical neutrality is maintained by conductive MWNT whose mobility is several orders higher in magnitude than that of polymer. Charge transfer and transport in ITO/MOPPV-MWNT:PCBM/PbSe/Al was illustrated by band energy diagram (Fig. 5). The favorable energy band alignment is advantageous to exciton dissociation, charge transfer and collection. Neutral excitons in MOPPV are dissociated from columbus attraction to electrons and holes at the interface. Efficient electron transfer from MOPPV, PCBM to PbSe, and collected by Al electrode is facilitated

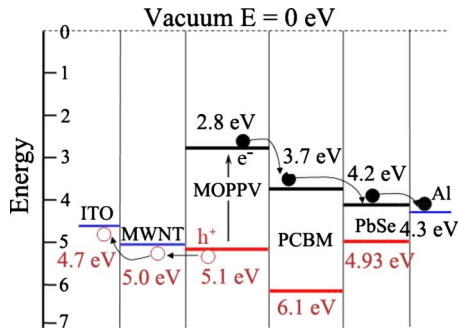


FIG. 5. (Color online) Energy level diagram adjusted in relation to the vacuum level for ITO/MOPPV-MWNT:PCBM/PbSe/Al OPV. Arrows indicate the electron and hole transport.

by the band edge offsets. MWNT with high carrier mobility primarily acts a metallic conductor and serves as an efficient nanoscale route for hole transfer and collection.¹⁵ Therefore, holes at HOMO of MOPPV are easily transferred to conduction band of PCBM because of low band gap. The transport pathway and a better ohmic contact between ITO and MWNT minimize charge recombination during transfer and hole extraction at the electrode. Furthermore, as shown in Fig. 2(b), interpenetrating network of well-dispersed MWNT in MOPPV matrix also contribute to the high performance of bulk heterojunction devices.¹⁶ Infiltration of PbSe QDs improves the intimate contact between QDs and polymer chains, and thus enhances the exciton dissociation. Consequently, high photovoltaic performance with twofold increase in J_{sc} and η results from efficient exciton dissociation, charge transfer and transport.

In summary, we fabricated a solution-processed bulk heterojunction OPV based on MOPPV-MWNT/PbSe bilayer. The interpenetrating network of well-dispersed MWNT covalently bonding to the MOPPV matrix facilitated the exciton dissociation and charge transfer by the infiltration of PbSe QDs. A dramatic twofold increase in J_{sc} (1.71 mA/cm²) and η (0.40%) was obtained in ITO/MOPPV-MWNT:PCBM/PbSe/Al device compared with that

without MWNT. The enhanced performance stemmed from the efficient excitation dissociation, charge transfer, and transport. Results indicated the photocurrent of MOPPV-MWNT OPV could be further improved by integration of conductive well-dispersed MWNT due to efficient charge transfer and high carrier mobility resulting in high photovoltaic performance.

This work was partly supported by the National Basic Research Program of China (Grant No. 2010CB934700) and the National Natural Science Foundation of China (Grant No. 50873074).

- ¹S. Na, S. S. Kim, J. Jo, and D. Y. Kim, *Adv. Mater.* **20**, 4061 (2008).
- ²H. Hoppe and N. S. Sariciftci, in *Photoresponsive Polymer II*, Advances in Polymer Science, edited by S. R. Marder and K. S. Lee (Springer, Berlin, 2008), Vol. 214, pp. 1–86.
- ³E. Kymakis and G. A. J. Amarantunga, *Appl. Phys. Lett.* **80**, 112 (2002).
- ⁴B. Pradhan, S. K. Batabyal, and A. J. Pal, *Appl. Phys. Lett.* **88**, 093106 (2006).
- ⁵D. M. N. M. Dissanayake, A. A. D. T. Adikaari, and S. R. P. Silva, *Appl. Phys. Lett.* **92**, 093308 (2008).
- ⁶R. D. Schaller, M. Sykora, J. M. Pietryga, and V. I. Klimov, *Nano Lett.* **6**, 424 (2006).
- ⁷G. I. Koleilat, L. Levina, H. Shukla, S. H. Myrskog, S. Hinds, A. G. Pattantyus-Abraham, and E. H. Sargent, *ACS Nano* **2**, 833 (2008).
- ⁸B. Vigolo, V. Mamane, F. Valsaque, T. N. H. Le, J. Thabit, J. Ghanbaja, L. Aranda, Y. Fort, and E. Mcare, *Carbon* **47**, 411 (2009).
- ⁹D. Q. Yun, W. Feng, H. C. Wu, B. M. Li, X. Z. Liu, W. H. Yi, J. F. Qiang, S. Gao, and S. L. Yan, *Synth. Met.* **158**, 977 (2008).
- ¹⁰A. Sashchiuk, L. Amirav, M. Bashouti, M. Krueger, U. Sivan, and E. Lifshitz, *Nano Lett.* **4**, 159 (2004).
- ¹¹H. Du, C. L. Chen, R. Krishnan, T. D. Krauss, J. M. Harbold, F. W. Wise, M. G. Thomas, and J. Silcox, *Nano Lett.* **2**, 1321 (2002).
- ¹²W. Feng, A. Fujii, M. Ozaki, and K. Yoshino, *Carbon* **43**, 2501 (2005).
- ¹³Z. A. Tan, T. Zhu, M. Thein, S. Gao, A. Cheng, F. Zhang, C. F. Zhang, H. P. Su, J. K. Wang, R. Herderson, J. Hahm, Y. P. Yang, and J. Xu, *Appl. Phys. Lett.* **95**, 063510 (2009).
- ¹⁴C. Melzer, E. J. Koop, V. D. Mihailtchi, and P. W. M. Blom, *Adv. Funct. Mater.* **14**, 865 (2004).
- ¹⁵S. Chaudhary, H. W. Lu, A. M. Muller, C. J. Bardeen, and M. Ozkan, *Nano Lett.* **7**, 1973 (2007).
- ¹⁶Y. Y. Feng, X. H. Ju, W. Feng, H. B. Zhang, Y. W. Cheng, J. Liu, A. Fujii, M. Ozaki, and K. Yoshino, *Appl. Phys. Lett.* **94**, 123302 (2009).